On-the-fly cross flow laser guided separation of aerosol particles based on size, refractive index and density–theoretical analysis

A. A. Lall,[1] A. Terray,[2] and S. J. Hart[*,2]

[1]*Excet, Inc., Springfield, Virginia, USA*
[2]*Chemistry Division, Naval Research Laboratory, Washington DC, USA*
**sean.hart@nrl.navy.mil; (202) 404-3361*

Abstract: Laser separation of particles is achieved using forces resulting from the momentum exchange between particles and photons constituting the laser radiation. Particles can experience different optical forces depending on their size and/or optical properties, such as refractive index. Thus, particles can move at different speeds in the presence of an optical force, leading to spatial separations. In this paper, we present a theoretical analysis on laser separation of non-absorbing aerosol particles moving at speeds (1-10 cm/sec) which are several orders of magnitude greater than typical particle speeds used in previous studies in liquid medium. The calculations are presented for particle deflection by a loosely focused Gaussian 1064 nm laser, which simultaneously holds and deflects particles entrained in flow perpendicular to their direction of travel. The gradient force holds the particles against the viscous drag for a short period of time. The scattering force simultaneously pushes the particles, perpendicular to the flow, during this period. Our calculations show particle deflections of over 2500 μm for 15 μm aerosol particles, and a separation of over 1500 μm between 5 μm and 10 μm particles when the laser is operated at 10W. We show that a separation of about 421 μm can be achieved between two particles of the same size (10 μm) but having a refractive index difference of 0.1. Density based separations are also possible. Two 10 μm particles with a density difference of 600 kg/m^3 can be separated by 193 μm. Examples are shown for separation distances between polystyrene, poly(methylmethacrylate), silica and water particles. These large laser guided deflections represent a novel achievement for optical separation in the gas phase.

OCIS codes: (140) Lasers and laser optics; (140.7010) Trapping

References and links

1. A. Ashkin, "Acceleration and trapping of particles by radiation pressure," Phys. Rev. Lett. **24**(4), 156–159 (1970).
2. T. Kaneta, Y. Ishidzu, N. Mishima, and T. Imasaka, "Theory of optical chromatography," Anal. Chem. **69**(14), 2701–2710 (1997).
3. S. J. Hart, A. Terray, K. L. Kuhn, J. Arnold, and T. A. Leski, "Optical chromatography of biological particles," Am. Lab. **36**, 13 (2004).
4. S. J. Hart, and A. V. Terray, "Refractive-index-driven separation of colloidal polymer particles using optical chromatography," Appl. Phys. Lett. **83**(25), 5316–5318 (2003).
5. S. B. Kim, J. H. Kim, and S. S. Kim, "Theoretical development of in situ optical particle separator: cross-type optical chromatography," Appl. Opt. **45**(27), 6919–6924 (2006).
6. T. Imasaka, Y. Kawabata, T. Kaneta, and Y. Ishidzu, "Optical chromatography," Anal. Chem. **67**(11), 1763–1765 (1995).
7. J. D. Taylor, A. Terray, and S. J. Hart, "Analytical measurement using optical chromatography," Proceedings of the SPIE - The International Society for Optical Engineering, 74000P (74007 pp.) (2009).

#135559 - $15.00 USD Received 23 Sep 2010; revised 10 Nov 2010; accepted 11 Nov 2010; published 6 Dec 2010

Report Documentation Page

Form Approved
OMB No. 0704-0188

1. REPORT DATE	2. REPORT TYPE	3. DATES COVERED
NOV 2010		**00-00-2010 to 00-00-2010**

4. TITLE AND SUBTITLE	5a. CONTRACT NUMBER
On-the-fly cross flow laser guided separation of aerosol particles based on size, refractive index and density-theoretical analysis	5b. GRANT NUMBER
	5c. PROGRAM ELEMENT NUMBER
6. AUTHOR(S)	5d. PROJECT NUMBER
	5e. TASK NUMBER
	5f. WORK UNIT NUMBER
7. PERFORMING ORGANIZATION NAME(S) AND ADDRESS(ES) **Naval Research Laboratory,Chemistry Division,Washington,DC,20375**	8. PERFORMING ORGANIZATION REPORT NUMBER
9. SPONSORING/MONITORING AGENCY NAME(S) AND ADDRESS(ES)	10. SPONSOR/MONITOR'S ACRONYM(S)
	11. SPONSOR/MONITOR'S REPORT NUMBER(S)

12. DISTRIBUTION/AVAILABILITY STATEMENT
Approved for public release; distribution unlimited

13. SUPPLEMENTARY NOTES

14. ABSTRACT

Laser separation of particles is achieved using forces resulting from the momentum exchange between particles and photons constituting the laser radiation. Particles can experience different optical forces depending on their size and/or optical properties, such as refractive index. Thus, particles can move at different speeds in the presence of an optical force, leading to spatial separations. In this paper, we present a theoretical analysis on laser separation of non-absorbing aerosol particles moving at speeds (1-10 cm/sec) which are several orders of magnitude greater than typical particle speeds used in previous studies in liquid medium. The calculations are presented for particle deflection by a loosely focused Gaussian 1064 nm laser, which simultaneously holds and deflects particles entrained in flow perpendicular to their direction of travel. The gradient force holds the particles against the viscous drag for a short period of time. The scattering force simultaneously pushes the particles, perpendicular to the flow, during this period. Our calculations show particle deflections of over 2500 μm for 15 μm aerosol particles, and a separation of over 1500 μm between 5 μm and 10 μm particles when the laser is operated at 10W. We show that a separation of about 421 μm can be achieved between two particles of the same size (10 μm) but having a refractive index difference of 0.1. Density based separations are also possible. Two 10 μm particles with a density difference of 600 kg/m3 can be separated by 193 μm. Examples are shown for separation distances between polystyrene, poly(methylmethacrylate), silica and water particles. These large laser guided deflections represent a novel achievement for optical separation in the gas phase.

15. SUBJECT TERMS

16. SECURITY CLASSIFICATION OF:			17. LIMITATION OF ABSTRACT	18. NUMBER OF PAGES	19a. NAME OF RESPONSIBLE PERSON
a. REPORT	b. ABSTRACT	c. THIS PAGE			
unclassified	**unclassified**	**unclassified**	**Same as Report (SAR)**	**16**	

8. A. Terray, J. Arnold, and S. J. Hart, "Enhanced optical chromatography in a PDMS microfluidic system," Opt. Express **13**(25), 10406–10415 (2005).
9. A. Terray, J. D. Taylor, and S. J. Hart, "Cascade optical chromatography for sample fractionation," Biomicrofluidics **3** (2009).
10. A. Ashkin, J. M. Dziedzic, J. E. Bjorkholm, and S. Chu, "Observation of a single-beam gradient force optical trap for dielectric particles," Opt. Lett. **11**(5), 288–290 (1986).
11. A. Ashkin, "Forces of a single-beam gradient laser trap on a dielectric sphere in the ray optics regime," Biophys. J. **61**(2), 569–582 (1992).
12. K. C. Neuman, and S. M. Block, "Optical trapping," Rev. Sci. Instrum. **75**(9), 2787–2809 (2004).
13. D. G. Grier, "A revolution in optical manipulation," Nature **424**(6950), 810–816 (2003).
14. J. Makihara, T. Kaneta, and T. Imasaka, "Optical chromatography Size determination by eluting particles," Talanta **48**(3), 551–557 (1999).
15. A. Ashkin, and J. M. Dziedzic, "Optical levitation by radiation pressure," Appl. Phys. Lett. **19**(8), 283 (1971).
16. A. Ashkin, and J. M. Dziedzic, "Optical levitation of liquid drops by radiation pressure," Science **187**(4181), 1073–1075 (1975).
17. M. D. Summers, J. Reid, and D. McGloin, "Optical guiding of aerosols," Proc. SPIE **6326**, U352–U359 (2006).
18. M. D. Summers, J. P. Reid, and D. McGloin, "Optical guiding of aerosol droplets," Opt. Express **14**(14), 6373–6380 (2006).
19. R. J. Hopkins, L. Mitchem, A. D. Ward, and J. P. Reid, "Control and characterisation of a single aerosol droplet in a single-beam gradient-force optical trap," Phys. Chem. Chem. Phys. **6**(21), 4924–4927 (2004).
20. L. Mitchem, and J. P. Reid, "Optical manipulation and characterisation of aerosol particles using a single-beam gradient force optical trap," Chem. Soc. Rev. **37**(4), 756–769 (2008).
21. H. Meresman, J. B. Wills, M. Summers, D. McGloin, and J. P. Reid, "Manipulation and characterisation of accumulation and coarse mode aerosol particles using a Bessel beam trap," Phys. Chem. Chem. Phys. **11**(47), 11333–11339 (2009).
22. J. B. Wills, K. J. Knox, and J. P. Reid, "Optical control and characterisation of aerosol," Chem. Phys. Lett. **481**(4-6), 153–165 (2009).
23. J. R. Butler, J. B. Wills, L. Mitchem, D. R. Burnham, D. McGloin, and J. P. Reid, "Spectroscopic characterisation and manipulation of arrays of sub-picolitre aerosol droplets," Lab Chip **9**(4), 521–528 (2009).
24. T. Imasaka, "Optical chromatography, optical funnel, and optical channel for evaluation of biological cells," Abstracts of Papers of the American Chemical Society **229**, 001-ANYL (2005).
25. A. Ashkin, and J. M. Dziedzic, "Optical trapping and manipulation of viruses and bacteria," Science **235**(4795), 1517–1520 (1987).
26. S. J. Hart, A. Terray, J. Arnold, and T. A. Leski, "Optical chromatography for concentration of biological samples," Proceedings of the SPIE - The International Society for Optical Engineering, 632612 (2006).
27. S. J. Hart, A. Terray, T. A. Leski, J. Arnold, and R. Stroud, "Discovery of a significant optical chromatographic difference between spores of Bacillus anthracis and its close relative, Bacillus thuringiensis," Anal. Chem. **78**(9), 3221–3225 (2006).
28. R. B. Fair, A. Khlystov, V. Srinivasan, V. K. Pamula, and K. N. Weaver, "Integrated chemical/biochemical sample collection, pre-concentration, and analysis on a digital microfluidic lab-on-a-chip platform," Proc. SPIE **5591**, 113–124 (2004).
29. T. Reponen, K. Willeke, S. Grinshpun, and A. Nevalainen, "Biological particle sampling," in *Aerosol measurement: Principles, techniques and applications*, P. A. Baron, and K. Willeke, eds. (John Wiley and Sons, Inc., 2001), pp. 751–778.
30. S. D. Noblitt, G. S. Lewis, Y. Liu, S. V. Hering, J. L. Collett, Jr., and C. S. Henry, "Interfacing microchip electrophoresis to a growth tube particle collector for semicontinuous monitoring of aerosol composition," Anal. Chem. **81**(24), 10029–10037 (2009).
31. S. B. Kim, H. J. Sung, and S. S. Kim, "Nondimensional analysis of particle behavior during cross-type optical particle separation," Appl. Opt. **48**(22), 4291–4296 (2009).
32. S. B. Kim, K. H. Lee, H. J. Sung, and S. S. Kim, "Nonlinear particle behavior during cross-type optical particle separation," Appl. Phys. Lett. **95**(26), 264101 (2009).
33. S. B. Kim, S. Y. Yoon, H. J. Sung, and S. S. Kim, "Resolution of cross-type optical particle separation," Anal. Chem. **80**(15), 6023–6028 (2008).
34. A. A. Lall, and S. K. Friedlander, "On-line measurement of ultrafine aggregate surface area and volume distributions by electrical mobility analysis: 1. Theoretical analysis," J. Aerosol Sci. **37**(3), 260–271 (2006).
35. A. A. Lall, X. F. Ma, S. Guha, G. W. Mulholland, and M. R. Zachariah, "Online nanoparticle mass measurement by combined aerosol particle mass analyzer and differential mobility analyzer: Comparison of theory and measurements," Aerosol Sci. Technol. **43**(11), 1075–1083 (2009).
36. A. A. Lall, W. Rong, L. Madler, and S. K. Friedlander, "Nanoparticle aggregate volume determination byelectrical mobility analysis: Test of idealized aggregate theory using aerosol particle mass analyzer measurements," J. Aerosol Sci. **39**(5), 403–417 (2008).
37. A. A. Lall, M. Seipenbusch, W. Z. Rong, and S. K. Friedlander, "On-line measurement of ultrafine aggregate surface area and volume distributions by electrical mobility analysis: Ii. Comparison of measurements and theory," J. Aerosol Sci. **37**(3), 272–282 (2006).

#135559 - $15.00 USD Received 23 Sep 2010; revised 10 Nov 2010; accepted 11 Nov 2010; published 6 Dec 2010

38. S. K. Friedlander, *Smoke, dust and haze: Fundamentals of aerosol dynamics* (Oxford University Press, Inc., New York, 2000).
39. S. B. Kim, and S. S. Kim, "Radiation forces on spheres in loosely focused gaussian beam: Ray-optics regime," J. Opt. Soc. Am. B **23**(5), 897–903 (2006).
40. A. A. Lall, A. Terray, and S. J. Hart, "On-the-fly cross flow laser guided separation of aerosol particles " Proceedings of the SPIE - The International Society for Optical Engineering **7762,** 77620W (Aug. 27, 2010), doi: 10.1117/12.860742.

1. Introduction

The use of a laser to separate non-absorbing microscopic particles is based on the momentum exchange between the particles and the photons constituting the laser radiation; the resulting force is called optical or radiation pressure [1]. Particles experience an optical force based on their intrinsic properties such as size [2], shape [3], and refractive index [4]. Separations performed using a mildly focused laser beam typically involve a counter propagating fluid flow, and this is termed optical chromatography (OC); when the fluid flow is perpendicular to the laser beam, the separation is termed as cross-type optical chromatography [5]. In OC, particles in the laser beam with varying properties move differentially against an opposing fluid flow and come to rest where the optic and fluidic forces balance [5,6]. Such laser separations of particles in aqueous suspension have been shown in a number of our previous studies [3,7–9].

The optical force or pressure exerted by a laser beam on particles is primarily studied and applied in liquids using optical trapping / tweezers [10–13] and has been used to determine particle size [14]. A smaller number of studies have reported the use of optical force in the gas phase, for example, levitation of airborne particles [15,16], and more recent studies on aerosol optical guiding [17,18], tweezing and manipulation [19–23]. A common thrust for optical trapping studies in liquids is that many analytical methods for detecting airborne biological micro-organism such as bacteria are based in liquid suspensions or involve wet-chemistry methods [24–28]. Thus for airborne particles an additional step is often needed for transferring aerosol particles into liquid suspensions. The airborne particles of interest are often collected and added to liquid by impingers, impactors [29] or growth tube like devices [30]. In such suspensions, the particle concentration is often low for analysis and requires additional offline processing. Thus, there is an interest in direct optical separation of airborne particles without undergoing liquid based sampling or separation methods. An additional advantage of direct aerosol particle interrogation is the potential ability to sort particles of interest and make real time decisions regarding particle identity and the need to collect the sample or not.

Toward these goals, we have extended our studies to particles suspended in a carrier gas as an "aerosol". From an optical force separation and physics perspective, a gaseous medium is advantageous over a liquid medium for two reasons: (a) the refractive index of a gas (for example, $n_{air} = 1$) is smaller than the refractive index of a liquid (for example, $n_{water} = 1.33$) which leads to greater optical force, (b) the viscous drag experienced by the particles in a gas is much smaller than the viscous drag in water.

In what follows, we first identify some key aspects of aerosols and aerosol sampling for cross-flow optical chromatography. Our goal is to use the newly developed theory to find appropriate parameters for the robust separation of aerosols based on size, refractive index and density.

1.1 Cross-flow optical chromatography

Kim et al. [5] introduced a novel concept termed *in situ* cross-type optical chromatography in water, where the laser beam is oriented perpendicularly to the fluid flow They derived an analytical solution for particle deflection using a spatially averaged scattering force which does not depend on particle position; the approximation can be made for laser beam width much larger than the particle size. Using the spatially averaged scattering force, Kim et al.

#135559 - $15.00 USD Received 23 Sep 2010; revised 10 Nov 2010; accepted 11 Nov 2010; published 6 Dec 2010

[31] and Kim et al. [32] postulated that the deflection is proportional to a non-dimensional number equal to the ratio of optical force to viscous drag; for higher values (>6), they found a non-linear relation.

A more accurate numerical solution for cross-flow optical separations, and comparison with measurements in liquid phase is given by Kim et al. [33]. In those experiments, 5 µm polystyrene (PS) particles moving at 300 µm/sec were deflected by about 20 µm using a 1W laser (λ = 532 nm, ω_0 = 40 µm). Higher particle flow rates are desirable for higher throughput but that leads to less deflection. In contrast to micro-fluidic channels, the particle velocity in typical aerosol sampling instruments is often several orders of magnitude higher. Despite higher particle velocities in the gas phase, the calculations presented in this paper indicate that a 5 µm PS particle moving at 300 × 10^2 µm/sec (3 cm/sec) can be deflected by over 1000 µm using a 10W laser (λ = 1064 nm, ω_0 = 10 µm). Thus a typical deflection in the gas phase is much greater than in the liquid phase, and at much larger throughput.

1.2 Relevance of Optical Chromatography for Bioaerosols

Commonly encountered bioaerosols are spores, pollen, viruses, bacteria and other particles of biological origin. The size ranges from tens of nanometers to tens of micrometers. It is estimated that about 30% of the particles larger than 200 nm in outdoor air are of biological origin [29]. Figure 1 shows different biological particles and their size range. Particles that are less than 5 µm in size have the longest airborne lifetime.

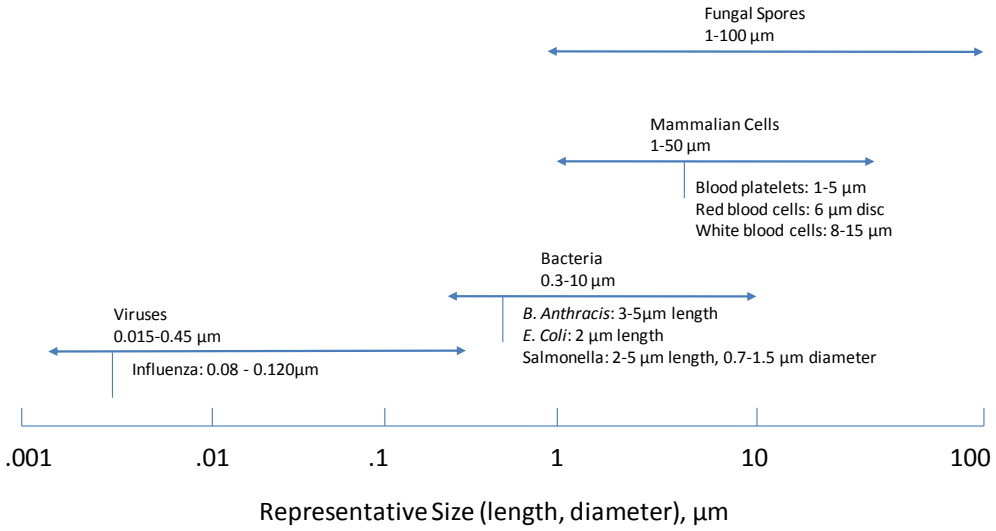

Fig. 1. Biological particle size chart. Particles of the same size can differ in density and / or refractive index.

Biological particles differ from inorganic particles of comparable size in terms of their density, refractive index, absorbance, and fluorescence characteristics. Traditional aerosol characterization methods such as the aerodynamic particle sizer (APS) are limited to differentiation based on aerodynamic size (regardless of shape), and some methods due to fluorescence characteristics. Other electrostatics based methods for size and density measurements such as the differential mobility analyzer and aerosol particle analyzer [34–37] are primarily used for submicron aerosols, require particle charging, and may need multiple charging correction for larger particle sizes. Thus the laser guided separation method may have the potential to be an all-in-one method for separations based on size, density and refractive index. Further experimental and theoretical analysis is needed to evaluate the efficacy of this method; the presented study is the first step towards this goal.

#135559 - $15.00 USD Received 23 Sep 2010; revised 10 Nov 2010; accepted 11 Nov 2010; published 6 Dec 2010

2. Theory

In this section, we describe equations governing the viscous and optical forces. The viscous drag on a particle is given by:

$$F_{drag} = 3\pi\mu D_p V / C_{cunningham}, \tag{1}$$

where, $C_{cunningham}$ is the Cunningham slip correction factor [38], μ is gas viscosity, D_p is particle diameter and V is particle velocity relative to the gas.

The optical force expression is given by Kim and Kim [39] using the ray optics approach. The two components of the optical force, $F_{scatter}$ and $F_{gradient}$ force are given by:

$$F_{scatter} = \frac{n_0}{2c}\int_0^{2\pi}\int_0^{\pi/2} I(r,z)\left[1+R\cos 2\theta_1 - T^2\frac{\cos 2(\theta_1-\theta_2)+R\cos 2\theta_1}{1+R^2+2R\cos 2\theta_2}\right](\frac{D_p}{2})^2 \sin 2\theta_1 d\theta_1 d\varnothing, \tag{2}$$

$$F_{gradient} = -\frac{n_0}{2c}\int_0^{2\pi}\int_0^{\pi/2} I(r,z)\left[1+R\sin 2\theta_1 - T^2\frac{\sin 2(\theta_1-\theta_2)+R\sin 2\theta_1}{1+R^2+2R\cos 2\theta_2}\right](\frac{D_p}{2})^2 \sin 2\theta_1 \cos\varnothing d\theta_1 d\varnothing, \tag{3}$$

where:

n_0 is the refractive index of the medium,

c is the speed of the light,

r is the radial offset of the sphere from the Gaussian beam center axis,

z is the axial distance from the minimum beam waist,

R is the Fresnel's coefficients of reflectance,

T is the Fresnel's coefficients of transmittance,

θ_1 is the incident angle of the photon stream with respect to the normal direction of the sphere surface,

θ_1 is the refraction angle

θ_2, obtained by Snell's law, $= \sin^{-1}\left(\frac{n_0}{n_2}\sin\theta_1\right)$

n_2 is the refractive index of the particle,

Ø is the polar angle,

and, $I(r,z)$ is the beam intensity profile given by,

$$I(\rho,z) = \frac{2P}{\omega(z)^2}\exp\left[-\frac{2r^2}{\omega(z)^2}\right], \tag{4a}$$

where P is the power of the beam, and $\omega(z)$ is the beam radius at the axial distance z, and expressed as

$$\omega(z) = \omega_o\left[1+\left(\frac{\lambda z}{\pi\omega_0^2}\right)^2\right]^{1/2}, \tag{4b}$$

where ω_o is the minimum beam waist diameter is given by

#135559 - $15.00 USD Received 23 Sep 2010; revised 10 Nov 2010; accepted 11 Nov 2010; published 6 Dec 2010

$$\omega_o = \frac{2\lambda}{\pi}\frac{F}{D_p}. \tag{4c}$$

The Fresnel coefficients of reflectance (R) and transmittance (T), are given by:

$$R = \frac{1}{2}\left[\frac{\sin^2(\theta_1-\theta_2)}{\sin^2(\theta_1+\theta_2)} + \frac{\tan^2(\theta_1-\theta_2)}{\tan^2(\theta_1+\theta_2)}\right], \tag{5a}$$

$$T = 1-R = \frac{1}{2}\left[\frac{\sin 2\theta_2 \sin 2\theta_1}{\sin^2(\theta_1+\theta_2)} + \frac{\sin 2\theta_2 \sin 2\theta_1}{\sin^2(\theta_1+\theta_2)\cos^2(\theta_1-\theta_2)}\right]. \tag{5b}$$

The equation of motion is given by:

$$m\cdot\vec{a} = \text{Net force on the particle} = \Delta\vec{F}. \tag{6a}$$

In the presence of an optical and viscous force, Eq. (6)a can be written as:

$$m\cdot\vec{a} = m\cdot\frac{d\vec{v}}{dt} = \vec{F}_{laser} + \vec{F}_{viscous} + \vec{F}_{gravitational}. \tag{6b}$$

Thus the particle motion in the beam (Fig. 2) is a complex interplay between rapidly changing laser scatter ($F_{scatter}$) and gradient forces ($F_{gradient}$) with the viscous forces due to the carrier gas. The scattering force pushes the particle in the horizontal direction, and the gradient force, $F_{gradient}$, acts in the vertical direction towards the middle of the beam. Both $F_{scatter}$ and $F_{gradient}$ are a function of particle size and refractive index. Thus, in principle, the particles that differ in size and refractive index can be separated.

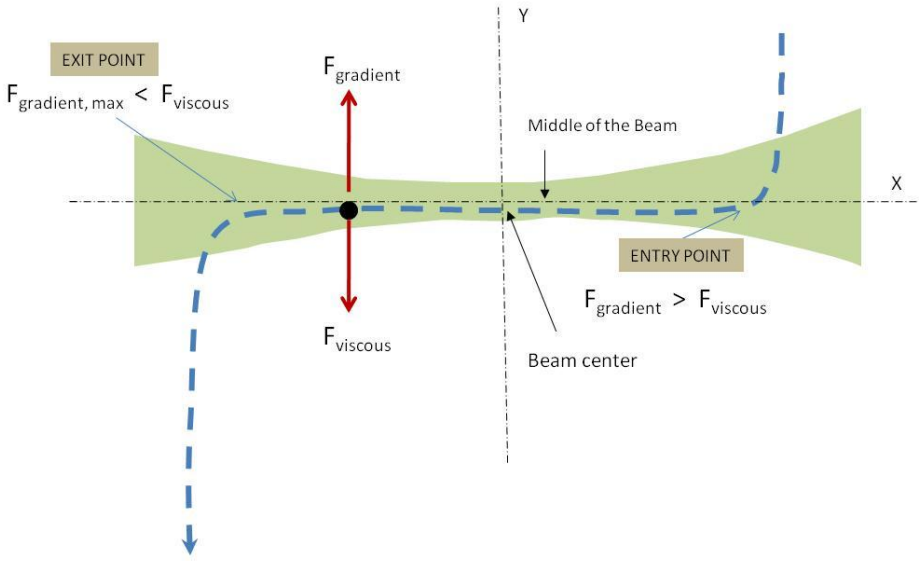

Fig. 2. Force balance in vertical and horizontal direction, and the resulting particle trajectory. The entry and exit points are determined by the balance between the viscous and gradient force.

Equation (6)b can be solved for x- and y- vectors. For the horizontal x-direction, the particle motion is described by:

$$\rho\frac{\pi D_p^3}{6}\cdot\frac{dv_x}{dt} = F_{scatter}(x,y) - 3\pi\mu D_p v_x. \tag{7}$$

To solve for particle trajectory, Eq. (7) can be written as:

#135559 - $15.00 USD Received 23 Sep 2010; revised 10 Nov 2010; accepted 11 Nov 2010; published 6 Dec 2010

$$\rho \frac{\pi D_p^3}{6} \cdot \frac{d^2 y}{dt^2} = F_{gradient}(x,y) - 3\pi\mu D_p \left(\frac{dy}{dt} - v_g \right) - \rho \frac{\pi D_p^3}{6} g. \quad (8)$$

In the vertical y-direction, the particle motion is described by,

$$\rho \frac{\pi D_p^3}{6} \cdot \frac{dv_y}{dt} = F_{gradient}(x,y) - 3\pi\mu D_p (v_y - v_g) - \rho \frac{\pi D_p^3}{6} g, \quad (9)$$

$$\rho \frac{\pi D_p^3}{6} \cdot \frac{d^2 y}{dt^2} = F_{gradient}(x,y) - 3\pi\mu D_p \left(\frac{dy}{dt} - v_g \right) - \rho \frac{\pi D_p^3}{6} g, \quad (10)$$

where g is the acceleration due to gravity (9.81 m/s^2). Equation (9) and 10 can be solved simultaneously using the numerical finite difference method. In the following calculations, the net particle deflection (δ) is recorded. The separation (S) between different particles (1 and 2) is given by:

$$S_{1,2} = \delta(D_{p,1}, n_{1,1}, \rho_1) - \delta(D_{p,2}, n_{1,2}, \rho_2). \quad (11)$$

3. Results and discussion

The horizontal force balance between laser scattering force and viscous force determines the deflection of the particle in the laser beam. The vertical balance of the laser gradient force and the viscous force determines the total residence time in the beam. The residence time determines how long the horizontal scattering force will act on the particle, and thereby affects deflection.

In this section, operating parameters affecting particle motion in the laser beam are studied. The parameters are:

a. Carrier gas vertical velocity, v_g (1-10 cm/sec)

b. Laser power, P (5-40W)

c. Laser beam minimum waist diameter, $2\omega_0$ (8-68 μm)

d. Gas and particle temperature, T = 298 K

Each of the above parameters is studied for a set of PS particle sizes (2-15 μm) and appropriate separation parameters are identified.

3.1 Effect of carrier gas vertical velocity

Figure 3 shows the particle trajectories for a 10 μm particle with vertical gas velocities of 1 to 9 cm/sec. The particle motion is described as follows: Consider the particle trajectory for 4cm/sec gas velocity. The particle enters the beam and is pushed downwards by the gradient force. As the particle passes through the middle (shown in Fig. 2) of the beam, the gradient force reverses its direction to oppose the particle vertical motion. At a low point in the particle trajectory (marked as A), the gradient force reduces the particle velocity to zero ($v_y = 0$) and the particle begins to move up ($F_{gradient} > F_{viscous}$). The particle in this condition is said to be retained vertically inside the beam. The greater gradient force pushes the particle towards the middle of the beam and the particle gains an upwards velocity ($v_y > 0$). Thus the particle no longer continues to move along with the gas. The particle then passes through the middle of the beam and its vertical travel is decelerated due to the gradient force acting downwards. At the point where the velocity reduces to zero the particle begins to accelerate downward. The particle exits the beam when the particle has moved far enough from the beam center such that the gradient force is no longer strong enough to counter the viscous force. The particle

#135559 - $15.00 USD Received 23 Sep 2010; revised 10 Nov 2010; accepted 11 Nov 2010; published 6 Dec 2010

was retained up to the gas speed of 6.5 cm/sec (shown as dashed line in Fig. 3). For higher gas speed ≥ 6.6 cm/sec (shown as dashed line in Fig. 3), the particle was merely deflected but not retained, or guided within the beam. In this case, the particle velocity in the Y- direction was always less than 0 ($v_y < 0$) suggesting that motion along the direction of gas flow was only reduced but not reversed. Using the above discussion, we define the condition for particle retention in the beam as $v_y \geq 0$.

The particle retention, upward particle movements inside the beam and millimeter scale deflections were observed in our previous experiments [40]. The theoretical analysis presented in this study explains the observed phenomena, which were not present in liquid phase experiments.

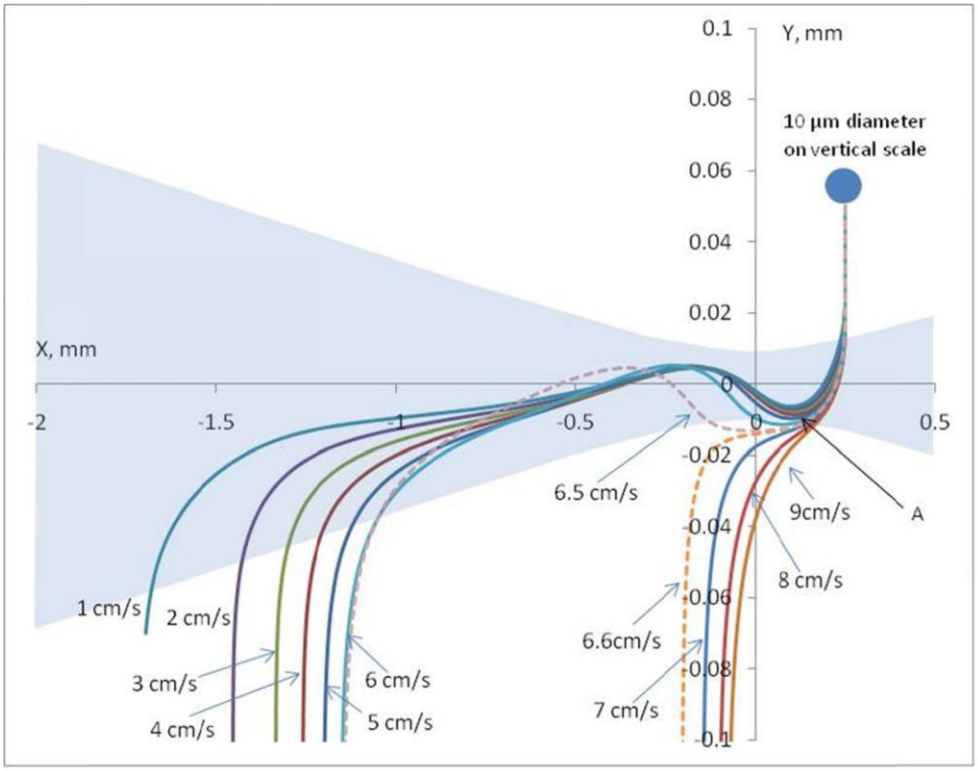

Fig. 3. Particle trajectories at different vertical gas speeds. Notice x- and y- axes are scaled differently for clarity. Particle diameter = 10 µm. Laser power = 10W. Minimum waist diameter = 20 µm (ω_0 = 10 µm). The center focal point and middle of the beam are located at (0, 0).

As discussed earlier, the particle trajectories can differ for different particle sizes. To determine the particle deflection (and thereby separation), we compared the particle trajectories of 2, 5 and 10 µm particles (as shown in Fig. 4). It is found that the 10 µm particle stays retained in the beam longer than the 5 µm particle. The 2 µm particle was merely deflected but not retained as the gradient force was not strong compared to the viscous drag. Furthermore, the larger particle travels farther in the beam than the small particle. A net separation (S) of over 1 mm is observed between 2 and 10 µm particles.

#135559 - $15.00 USD Received 23 Sep 2010; revised 10 Nov 2010; accepted 11 Nov 2010; published 6 Dec 2010

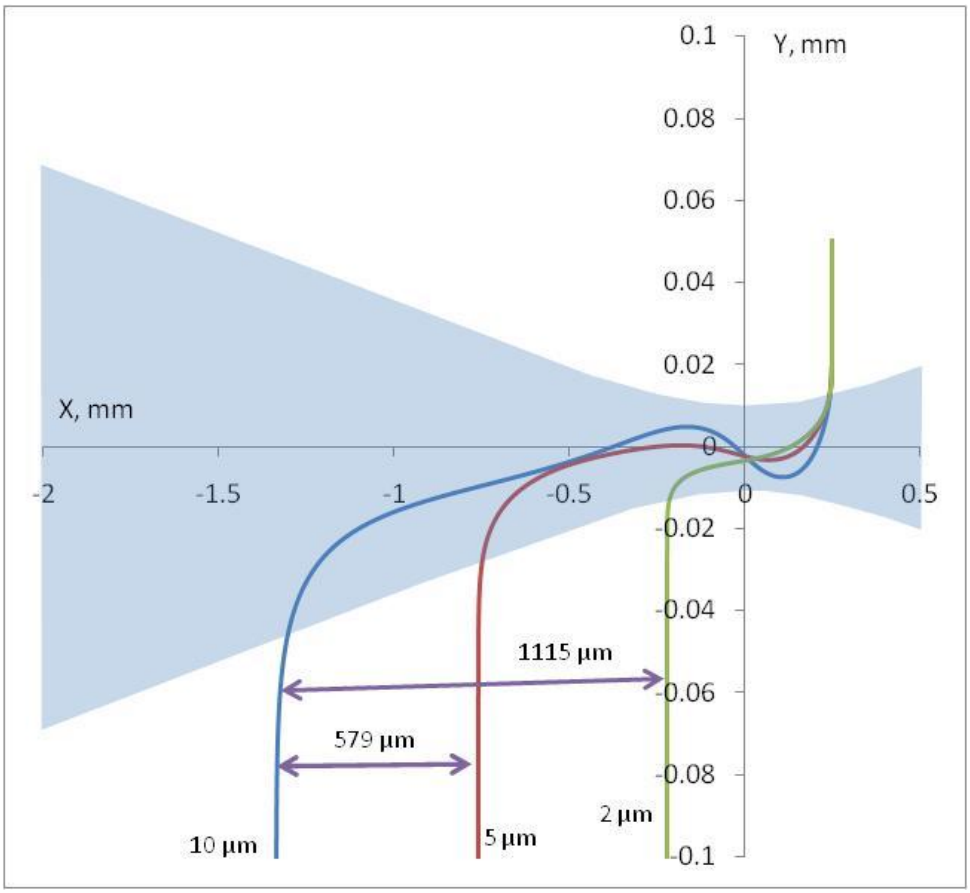

Fig. 4. Particle trajectories for 2, 5 and 10 µm PS particles. Notice x- and y- axes are scaled differently for clarity. Laser power = 10W. Minimum beam waist diameter = 20 µm (ω_0 = 10 µm). The center focal point and middle of the beam are located at (0, 0). Gas velocity = 3 cm/sec.

3.2 Effect of laser power and minimum beam waist diameter

Figure 5 shows the net deflection for 2, 5, 10 and 15 µm particles as a function of laser power. As expected, the particles were retained longer and deflected more at higher laser power. The calculations show that a 10 micron particle can be deflected by about 2 mm using a 20W laser. High power multimode fiber lasers (nLight, Inc., Vancouver, WA) are currently being adapted for this purpose by our group.

#135559 - $15.00 USD Received 23 Sep 2010; revised 10 Nov 2010; accepted 11 Nov 2010; published 6 Dec 2010

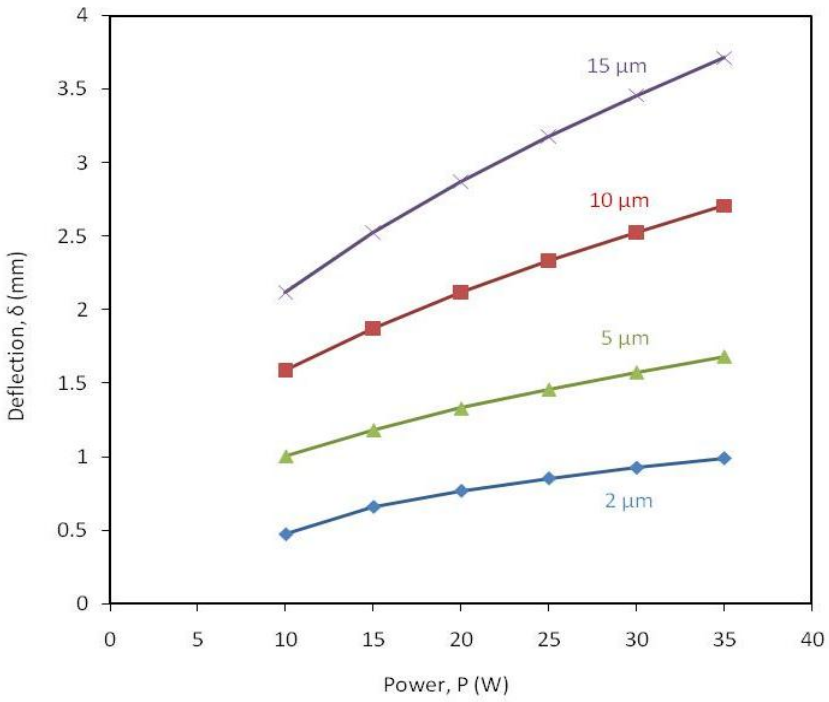

Fig. 5. Net deflection (δ) for 2, 5, 10 and 15 µm PS particles as a function of laser power. Minimum beam waist diameter = 20 µm (ω_0 = 10 µm). Gas velocity = 3 cm/sec.

Another way to increase the deflection is to decrease the minimum beam waist diameter ($2\omega_0$), thereby increasing the optical density and thus, the optical force. Therefore, to find an optimum condition, we varied the minimum beam waist diameter for a given laser power. Figure 6 shows net deflection for 5, 10 and 15 µm particles as a function of minimum beam waist diameter. Separation (S) between 5 and 10 µm particles, and 15 and 10 µm particles are shown in Fig. 6(b). We found that the new deflection initially increases with minimum beam waist diameter, reaches a maximum value and then drops down. The deflection at higher ω_0 decreases because particles are no longer vertically retained in the beam as the power density gets smaller. The maximum deflections were 1.04, 1.88 and 2.63 mm for 5, 10, and 15 µm particles, respectively.

As can be seen in Fig. 6a and 6b, a separation can be achieved when (a) both particles are retained (e.g., between 5 and 10 µm particles at ω_0 = 10 µm), (b) when one particle is retained and the other one is merely deflected (e.g., between 15 and 5 µm particles at ω_0 = 20 µm), and (c) when both particles are merely deflected (e.g., between 15 and 5 µm particles at ω_0 = 30 µm).

#135559 - $15.00 USD Received 23 Sep 2010; revised 10 Nov 2010; accepted 11 Nov 2010; published 6 Dec 2010

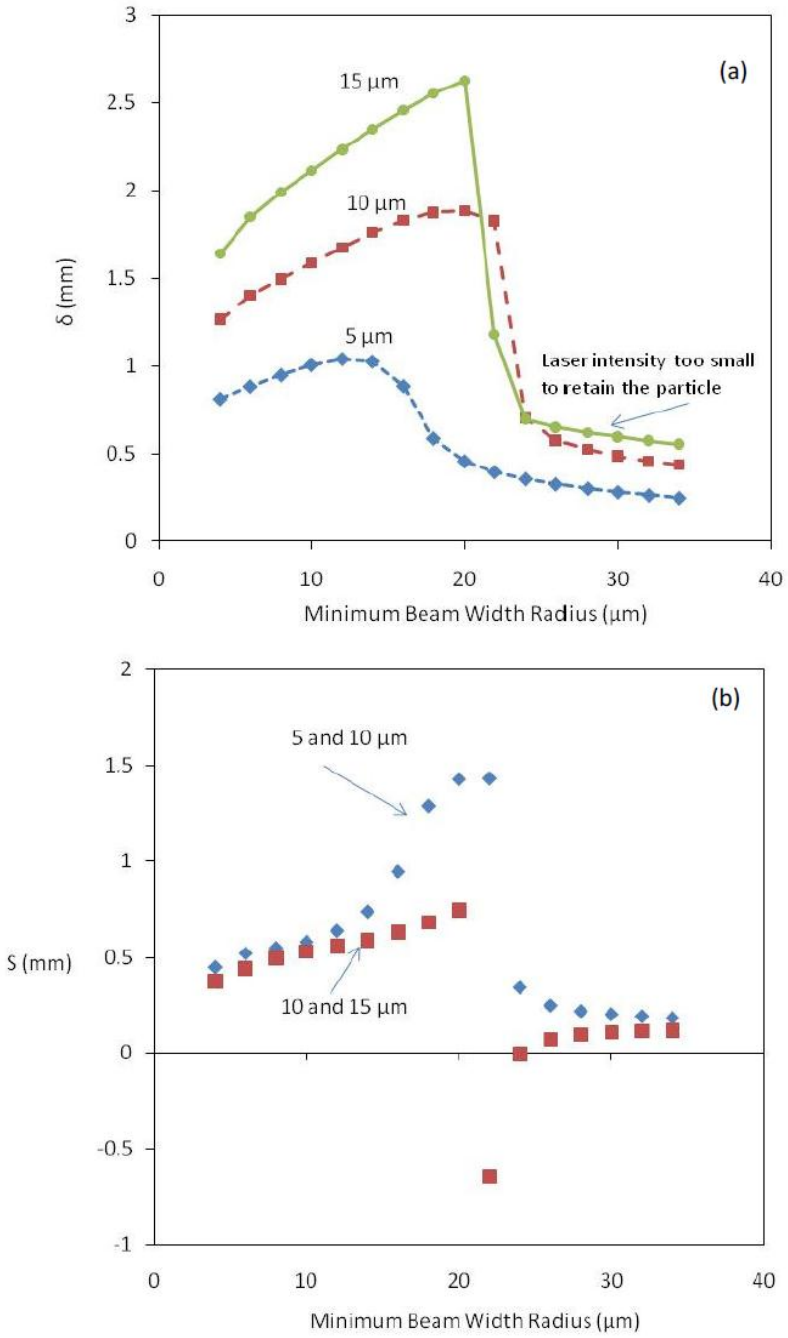

Fig. 6. (a) Net deflection for 5, 10 and 15 µm PS particles as a function of minimum beam width radius. (b) Separation (S) as a function of minimum beam width radius. Laser power = 10 W. Gas velocity = 3 cm/sec.

3.3 Separation between same size particles with different properties

In previous sections, we show that the separation distances were reasonably large for size based separations (Fig. 4-6). While particle sizes can differ in a wide range over several micrometers, properties such as refractive index and density often vary over a narrow range.

#135559 - $15.00 USD Received 23 Sep 2010; revised 10 Nov 2010; accepted 11 Nov 2010; published 6 Dec 2010

In this section, we investigate whether small variations in properties (refractive index and density) can lead to separation distances which can be used in practice for collection.

The minimum separation distance that is needed for an effective spatial differentiation is roughly about 10 times the particle size. About 100-150 microns separation can be considered reasonable for collection using typical aerosol instrumentation such as ¼" inch diameter tube with wall thickness of 0.127 mm, or using 1/10 thick metal plates/foils, which are available in a standard hardware store. More precise custom-made instrumentation, such as a knife edge may allow collection when the separation distances are smaller than 100 µm.

3.3.1 Separation based refractive indices

We investigated if it is possible to separate particles with only a small variation in their refractive indices which is often the case with biological particles. Figure 7 shows particle deflection for 2, 5 and 10 µm particles as a function of refractive index, for laser power = 40W and minimum beam waist radius (ω_0) = 4 µm. Example separations are 421 and 198 µm, for 10 and 5 µm particles respectively, when the refractive index difference was 0.1.

Our calculations show that it is possible to separate particles by about 200 µm when the difference in refractive indices is only 0.1. The separation is a strong function of minimum beam waist radius and laser power. An appropriate combination of laser power and minimum beam waist radius can be found using the above method.

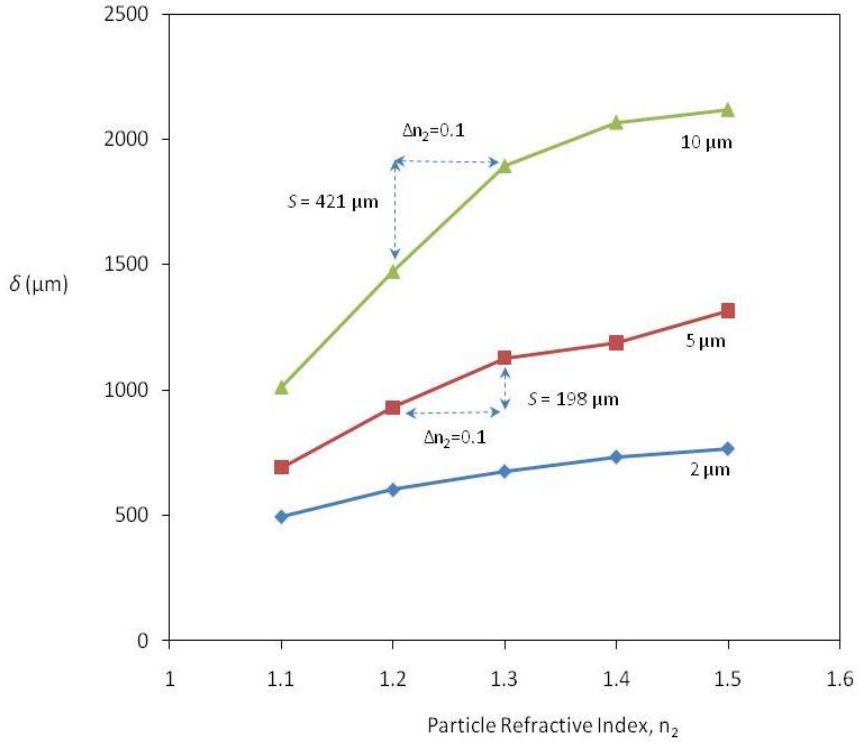

Fig. 7. Particle deflection for 2, 5 and 10 µm particles as a function of refractive index. Laser power = 40W. Minimum beam waist radius (ω_0) = 4 µm. Gas velocity = 3 cm/sec. Particle density = 1000 kg/m^3. Example separations are 421 and 198 µm for 10 and 5 µm particles respectively, when the refractive index difference was 0.1.

#135559 - $15.00 USD Received 23 Sep 2010; revised 10 Nov 2010; accepted 11 Nov 2010; published 6 Dec 2010

3.3.2 Separation based on densities

Particles such as silica, water droplets, biological particles, PS, poly(methyl methacrylate) (PMMA) differ in refractive indices and/or densities. To investigate the effect of particle density alone, we chose hypothetical particles with refractive index of 1.59 and varied the particle density from 1000 to 2000 kg/m^3. Figure 8 shows particle deflection for 2, 5 and 10 µm particles as a function of particle density at laser power = 10W and minimum beam waist radius (ω_0) = 4 µm. The figure shows the particles that differ in density alone can be separated, for example, 10 µm particles with a density difference of 600 kg/m^3 can be separated by 193 µm, and 5 µm particles can be separated by 143 µm for a density difference of 1000 kg/m^3.Thus we conclude that particle inertia may play a small but important role when precision separations are needed.

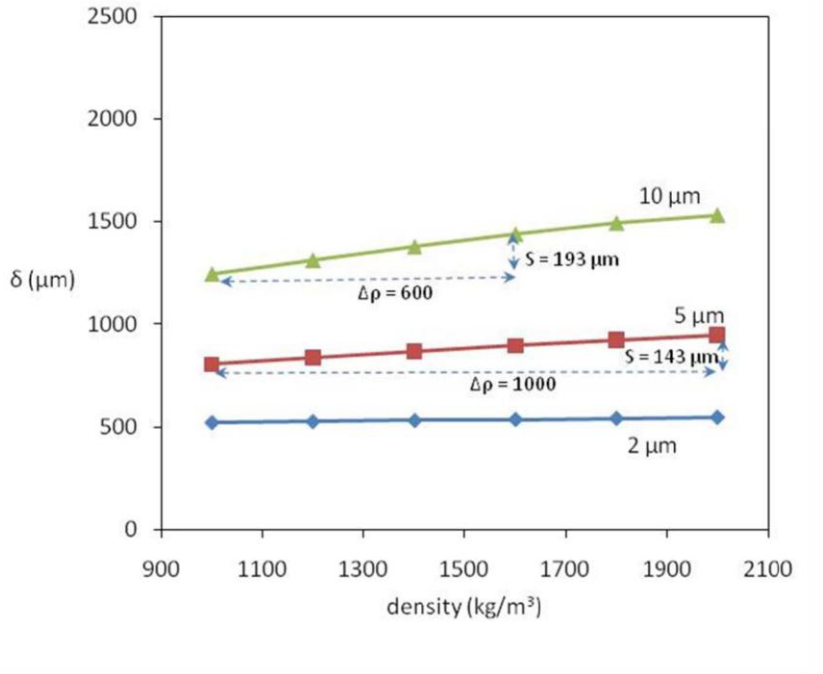

Fig. 8. Particle deflection for 2, 5 and 10 µm particles as a function of particle density. Laser power = 10W. Minimum beam waist radius (ω_0) = 4 µm. Gas velocity = 3 cm/sec. Particle refractive index = 1.59. Example separations: For 10 µm particle, the separation is 193 µm for a density difference of 600 kg/m^3. For 5 µm particle, the separation is 143 µm for a density difference of 1000 kg/m^3.

3.4 Separation distance between realistic particles: PS, PMMA, silica and water

In previous sections, we discussed the effect of certain particle properties on particle deflection, and estimated whether the separation was possible for a given difference in particle properties. Real particles, on the other hand, differ in more than one property, size, refractive index and density. So in this section, we considered examples of realistic particles and calculated the separation distance for various conditions.

Figure 9 shows deflection as a function of laser power for realistic 5 µm particles having density and refractive index of silica, PS, PMMA and water particles. The particle velocities prior to entering the beam (about 3 cm/sec) were several orders of magnitudes higher than the velocities typically used in liquid phase cross flow separations (about µm/sec). This implies that higher power is needed to deflect the particles. However, we show that despite high speed of 3 cm/sec, there is a considerable macroscopic separation between the particles (Fig. 9) at

#135559 - $15.00 USD Received 23 Sep 2010; revised 10 Nov 2010; accepted 11 Nov 2010; published 6 Dec 2010

laser power as low as 10W. For example, separation between silica and water particles was over 100 µm at 10W. Higher power leads to larger separation between particles in most cases. Table 1 shows the separation distance between particles at laser power = 40W, and minimum beam waist radius of 4 µm. These separation distances were reasonably large, and larger separation distances can be achieved when the laser power is increased. The limitation, however, may be the ability of the particle to withstand the damage in the laser beam; a greater convective dissipation of energy by gas molecules may help to avoid damage. Controlling power density may alleviate some issues but further studies are needed.

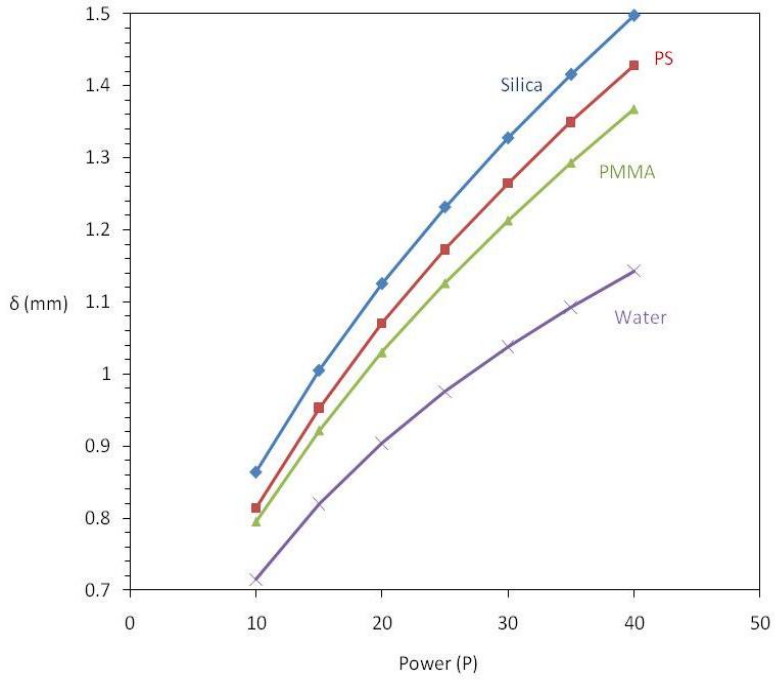

Fig. 9. Deflection for realistic particles having density and refractive index of silica, PS, PMMA and water particles. Both density and refractive index contribute to the deflection and resulting separation between the particles. Particle diameter = 5 µm. Minimum beam waist radius, ω_0 = 4 µm. Vertical gas velocity = 3 cm/sec.

Table 1. Separation distances for realistic 5 µm particles having properties close to silica, PS, PMMA and water particles. Laser Power = 40W, ω_0 = 4 µm.

Particle Properties			Separations (µm)			
Type	**RI**	**Density (kg/m^3)**	**Silica**	**PS**	**PMMA**	**Water**
Silica	1.43	2000	0	69.1	130	354
PS	1.59	1050	69.1	0	60.5	285
PMMA	1.49	1200	130	60.5	0	225
Water	1.33	1000	354	285	225	0

While higher power leads to larger separation in general, we can make use of complex particle motion characteristics for achieving larger separation distances at lower laser power values (~5W) as follows. One can use the above theory to calculate a condition in which one particle gets retained in the beam while other merely gets deflected but does not get retained in the beam. For example, a separation between 5 µm PS and PMMA particles is shown in Fig. 10 (Laser power = 5 W. Minimum beam waist radius, ω_0 = 4 µm. Vertical gas velocity =

#135559 - $15.00 USD Received 23 Sep 2010; revised 10 Nov 2010; accepted 11 Nov 2010; published 6 Dec 2010

4 cm/sec). The PS particle experiences a higher gradient force due to higher refractive index and is retained in the beam. For PMMA particles, the conditions were such that the gradient force was not sufficiently high to overcome the viscous drag and thus the PMMA particle was not retained. The resulting separation was 409 µm, much higher than the separation distance at higher laser power (at 10W). While in this example, we found these conditions by using a trial and error method to find a large separation distance, a careful selection of operating conditions for several different types of particles can be made using more rigorous optimization methods.

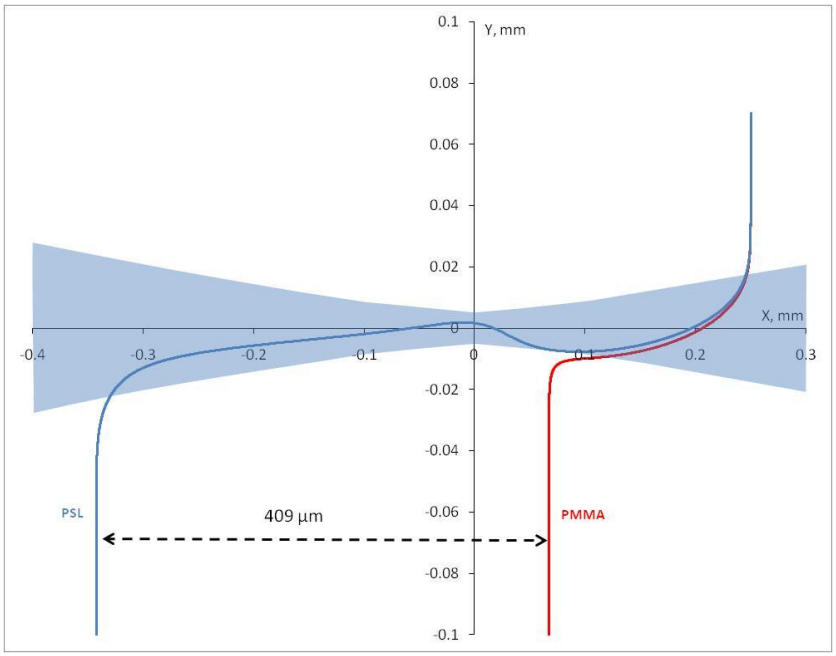

Fig. 10. Separation between PS and PMMA particles at a condition when the PS particle is retained in the beam (higher refractive index leading to higher gradient force) whereas the PMMA particle was not retained due to lower gradient force. Particle diameter = 5 µm. Laser power = 5 W. Minimum beam waist radius, ω_0 = 4 µm. Vertical gas velocity = 4 cm/sec.

4. Conclusions

Our study provides a theoretical starting point for on-the-fly laser separation of aerosols based upon operating parameters, i.e., laser power (~10W), minimum beam waist diameter (~4-40 µm), and aerosol flow rate (1-10 cm/sec). In this novel method, the gradient force resulted in the temporary retention of the particles while the scattering force pushed the particles perpendicular to the flow direction. Our theoretical calculations show that the particles in the size range of 1-15 microns can be separated by distances of up to a few millimeters based on size and optical properties. We report a separation of 1115 µm between 2 and 10 µm particles moving at 3 cm/sec (a typical laboratory aerosol flow rate) and at a laser power of 10W and minimum beam waist diameter of 20 µm. The large deflection values (over 1000 microns) that our method generates can be useful for separation of non-absorbing particles including biological particles.

Acknowledgments

The authors would like to acknowledge funding by the Defense Threat Reduction Agency (DTRA) under contract number BA09DET067, and the Naval Research Laboratory (NRL).

#135559 - $15.00 USD Received 23 Sep 2010; revised 10 Nov 2010; accepted 11 Nov 2010; published 6 Dec 2010

About Defense Threat Reduction Agency

The Defense Threat Reduction Agency (DTRA) was founded in 1998 to integrate and focus the capabilities of the Department of Defense that address the weapons of Mass Destruction (WMD) threat. The mission of the DTRA is to safeguard America and its allies from WMD threat (e.g. chemical, biological, radiological, nuclear and high yield explosives) by providing capabilities to reduce, eliminate and counter the threat and mitigate its effects. Under DTRA, Department of Defense resources, expertise and capabilities are combined to ensure the United States remains ready and able to address the present and future WMD threats. For more information on DTRA, visit www.dtra.mil/.

#135559 - $15.00 USD Received 23 Sep 2010; revised 10 Nov 2010; accepted 11 Nov 2010; published 6 Dec 2010